Effect of the spin-orbit interaction in photoionization Stark spectra of $m_l = 1$ excited rubidium atoms

J. M. Lecomte, S. Liberman, E. Luc-Koenig, J. Pinard, and A. Taleb
Laboratoire Aimé Cotton (Laboratoire associé à l'Université de Paris—Sud)
Centre National de la Recherche Scientifique II, Bâtiment 505, F-91405 Orsay Cedex, France
(Received 16 February 1983)

Experimental results on the photoionization spectra of excited rubidium atoms in a well-defined $m_l = 1$ state in the presence of an electric field are reported. Spectra corresponding to a definite polarization of the ionizing light exhibit characteristic resonances which are ascribed either to the non-Coulombic part of the central potential or to the spin-orbit interaction. The different line profiles are interpreted as being due to interferences between discrete states and continua, the observed structures depending directly on the density of oscillator strengths and not simply on the density of continuum states.

I. INTRODUCTION

Since the first observation of electric field induced resonances above the zero-field-ionization limit in the photoionization spectrum of atomic rubidium,[1,2] a lot of attention has been paid to photoionization Stark spectra of one-electron atoms both theoretically[3–5] and experimentally.[6–8] The structure of the Stark spectrum of hydrogen is theoretically well known because the corresponding Hamiltonian is separable in parabolic coordinates,[9] and thus the problem can be exactly solved. In the energy range extending from the classical field-ionization limit up to approximately the zero-field-ionization threshold, this spectrum consists of quasidiscrete states superimposed on continuum states. Because of the supersymmetry of the nonrelativistic Coulomb-Stark potential[10] there is no interaction between the quasistable states and the ionization continua. The quasidiscrete states have a very small width related to the probability of ionization by the tunneling of the electron through the potential barrier. When a perturbation breaks this symmetry a different field-ionization process occurs:[11] States which are stable with respect to the tunneling process can ionize through the mixing with an already ionizing state. The coupling leads to a broadening of the quasidiscrete states and, because of interference effects, it manifests itself in the appearance of asymmetric Fano profiles.[12] In a light alkali-metal atom the Rydberg-state electron experiences a non-Coulombic central potential and, in the Stark photoionization spectra, there exists a coupling between the quasidiscrete states and the underlying ionization continua having the same orbital magnetic quantum number m_l. This phenomenon has been observed in the Stark photoionization spectra of the sodium atom.[7,8] Furthermore, striking perturbations due to the Earth's magnetic field have been observed,[8] which demonstrates that very weak interactions can strongly perturb photoionization spectra. Indeed, even if it is weak, any interaction which couples a discrete state to a continuum completely modifies the ionization properties of the stable state. It is the aim of the present paper to point out that, in the rubidium atom, the spin-orbit interaction is sufficiently large to lead to the observation of additional structures in Stark photoionization spectra even near the zero-field-ionization limit. The spin-orbit interaction couples states with the same total magnetic quantum number m_j but with different m_l values. The importance of the spin-orbit interaction in the Stark photoionization spectra of rubidium has been observed previously in the energy range close to the classical field-ionization limit, where a very narrow Fano profile has been recorded.[13] The width of this profile was so small that this structure is likely to be attributed to the spin-orbit interaction. Another striking perturbation due to the spin-orbit interaction in the rubidium atom is the field-induced stabilization of a Stark state.[14] Lastly, it has been shown that, due to the spin-orbit interaction, it is more difficult to use the field-ionization technique as a highly selective detection method for a heavy alkali-metal atom such as rubidium.[15]

II. TWO-STEP STARK PHOTOIONIZATION SPECTRA OF THE RUBIDIUM ATOM

A. Experimental setup

The experimental setup used to study the photoionization Stark spectra of excited rubidium atoms in a well-defined $m_l = 1$ state is identical to the one used in a similar experiment on the sodium atom and is described somewhere else.[8] In these experiments a great deal of attention has been paid to rigorously define a pure m_l lower state as well as to precisely determine the polarization of the photoionizing light. Zeeman optical pumping is thus used to selectively populate the $5^2P_{3/2}$, $F = 4$, $M_F = 4$ state of the ^{85}Rb isotope, which corresponds to well-defined quantum numbers $m_l = 1$, $m_s = \frac{1}{2}$. An atomic beam of the natural mixture (72% of ^{85}Rb and 28% of ^{87}Rb) is subjected at the right angle to the interaction of the light of a cw single-mode dye laser which is right-hand circularly polarized. The hyperfine structures of both the ground state

and the excited state of the two isotopes are well resolved, and the laser is tuned and servo-locked on the transition $5^2S_{1/2}$, $F=3-5$ $^2P_{3/2}$, $F=4$ of the isotope ^{85}Rb. So the use of a cw laser permits the excitation of rubidium atoms in the pure $F=M_F=4$ substate. In order to check the good definition of the quantum numbers $m_l=1$, $m_s=\frac{1}{2}$, $m_j=\frac{3}{2}$, $M_F=4$ of the intermediate state, two experiments have been performed similarly to those done in the study of the sodium atom.[8] By using the field-ionization-detection technique we have recorded the unperturbed Rydberg spectra excited from the intermediate state by absorption of polarized light: In the σ^+ configuration only d states were observed, but in the σ^- configuration both s and d states were recorded. We have also verified that the critical ionizing energy values in the photoionization spectra depend on the polarization σ^+, π, or σ^- of the photoionizing light. Such observations make it possible to assert that the intermediate state is a pure $m_l=1$ state.

The photoionizing light is provided by a nitrogen-pumped pulsed dye laser, which counter propagates collinearly either with the exciting light or with the atomic beam. Consequently, the atoms excited in the $5^2P_{3/2}$, $m_l=1$ state are photoionized by a well polarized light, respectively (σ^+ or σ^-), and π according to the two possible propagation directions of the laser light.

The interaction region is located between the two grids of a capacitor. The ions produced are accelerated by the dc electric field and are extracted through the grids towards an electron multiplier.

In the present experiment the Earth's magnetic field, which was measured to be of 0.8 G in the interaction region, has been reduced to less than 0.02 G in the interaction region by using a pair of Helmholtz coils. Consequently, spurious symmetry breaking effects due to the presence of an additional external field are avoided.[8]

The Zeeman optical pumping is performed in the presence of an external electric field $\mathcal{F}=9950$ V/cm which partially destroys the atomic alignment obtained in the $5^2P_{3/2}$ level. However, the perturbation of the $5^2P_{3/2}$ level by the neighboring $4^2D_{3/2}$ and $5^2S_{1/2}$ levels due to the linear Stark effect is negligible, the mixing between these levels remaining smaller than 5×10^{-4} for the utilized field strength. Consequently, no significant symmetry breaking coming from Stark mixing exists in the intermediate state. Furthermore, the hyperfine interaction cannot perturb the intermediate state inasmuch as the extreme F value ($F=4$) associated with the 5^2P term is studied. In conclusion the Zeeman optical pumping process allows us to excite the ^{85}Rb atoms in the perfectly determined state 5^2P, $m_s=\frac{1}{2}$, $m_l=1$, $m_j=\frac{3}{2}$, $m_I=\frac{5}{2}$, $m_F=4$.

B. Experimental results

Using the above-described experimental setup, the photoion current has been recorded versus the pulsed laser frequency for the three polarizations of the photoionizing light. The results are presented in Fig. 1. The studied energy range is located in the vicinity of but below the zero-field-ionization limit. The three spectra correspond to the field strength $\mathcal{F}=9950$ V/cm. As one can see, they depend strongly on the polarization of the photoionizing light. The spectra are denoted, respectively, by $\sigma^+\sigma^-$, $\sigma^+\pi$, and $\sigma^+\sigma^+$ according to the polarizations of the exciting light and of the photoionizing light.

Structures still remain in the vicinity of the zero-field-ionization limit only in the $\sigma^+\sigma^-$ spectrum. These structures are relatively broad, and asymmetrical. With decreasing energy some of them appear to be narrower and more symmetrical; they can then be classified in two distinct groups. Indeed for $E\sim-200$ cm^{-1} one observes a staggering of broad and narrow resonances.

No structure appears in the $\sigma^+\pi$ spectrum at energy greater than -125 cm^{-1}. For lower energy values, some broad structures appear and they are followed by two series of resonances: one with narrow and symmetrical peaks and another one with broad and slightly asymmetrical resonances. The widths of the two types of structures are of the same order of magnitude in the $\sigma^+\sigma^-$ and $\sigma^+\pi$ spectra.

The $\sigma^+\sigma^+$ spectrum is quite different from the two others: no structure is observed in a very large energy range ($E>-220$ cm^{-1}). For a lower energy range very narrow and asymmetrical structures appear; they look like Fano profiles with a factor q of the order unity.[12] Between two such "dispersion curves" there is a sharp, narrow, and symmetrical resonance.

The three spectra $\sigma^+\sigma^-$, $\sigma^+\pi$, and $\sigma^+\sigma^+$ are very different ones from the others, especially in the energy range $E>-200$ cm.$^{-1}$ This proves again that the intermediate state $5^2P_{3/2}$ is a pure $m_l=1$ state; otherwise the $\sigma^+\sigma^+$ spectrum would have been polluted by resonances in the vicinity of the zero-field-ionization limit. The lack of structures in the $\sigma^+\pi$ spectrum at $E>-100$ cm^{-1}, and in the $\sigma^+\sigma^+$ spectrum at $E>-200$ cm^{-1} can be interpreted in the hydrogenic model. From the nonperturbative solution of the Schrödinger equation describing the hydrogen Stark effect,[4] we have determined the position, width, and partial density of states associated with the resonances located nearest to the zero-field-ionization limit, for states $|m_l|=0$, 1, and 2 which can be observed in the $\sigma^+\sigma^-$, $\sigma^+\pi$, and $\sigma^+\sigma^+$ spectra, respectively. Results are presented in Table I. In hydrogen, relatively narrow structures ($\Gamma<1$ cm^{-1}) are predicted near the zero-field-ionization limit, but the most excited resonances correspond to states $m_l=0$. Broader structures are associated with smaller density of excited states; consequently, they correspond to a small probability of excitation by absorption from the lower state $5^2P_{3/2}$ and they are not observed in the photoionization spectrum.

By comparing the three spectra, one can remark that some resonances appear in the spectra approximately at the same energy, but they have quite different widths and profiles. For example, the narrow resonances appearing in the $\sigma^+\sigma^-$ spectrum at $E\sim-200$ cm^{-1} are degenerate with the broad structures of the $\sigma^+\pi$ spectrum.

C. Identification of the resonances: Importance of the spin-orbit interaction

From the analysis of the experimental data, it has been shown that it is possible to classify the structures of a

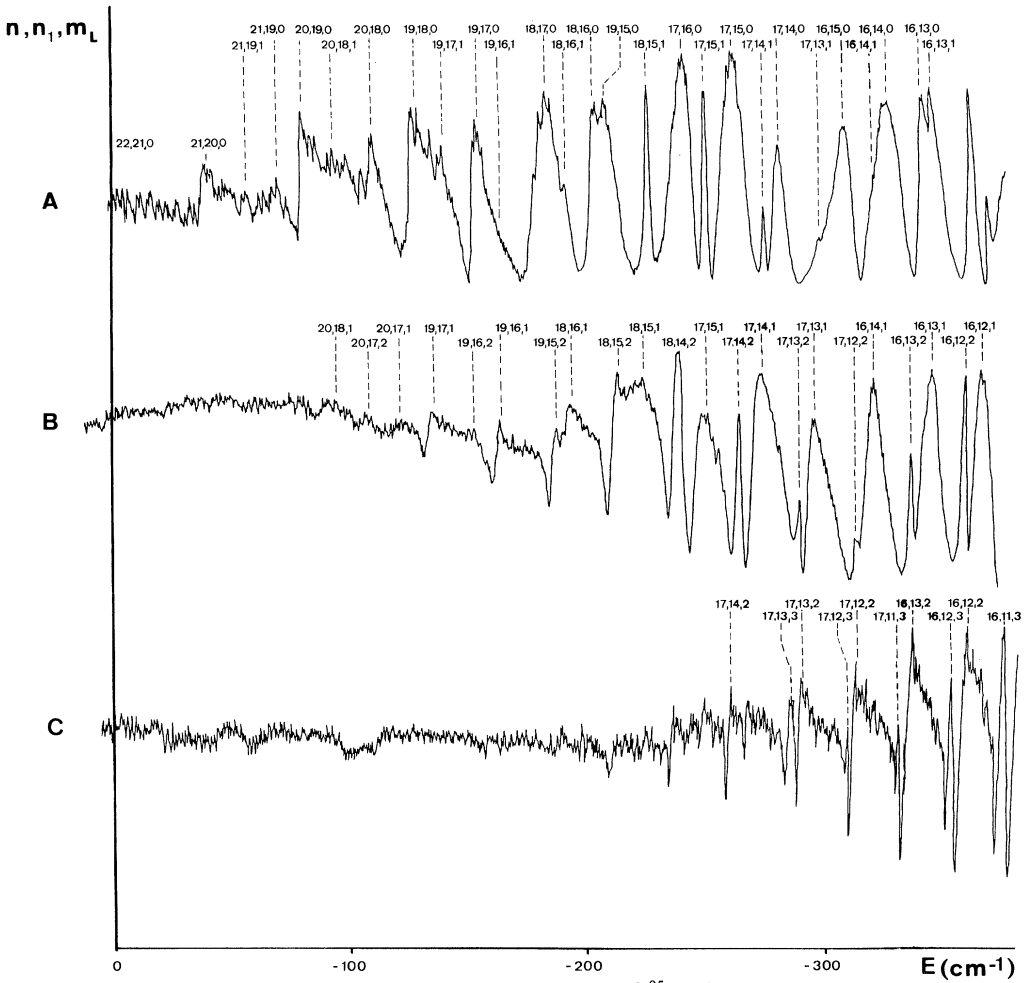

FIG. 1. Recording two-step photoionization spectra of the ground state of ^{85}Rb for various light polarizations and for the field strength $\mathcal{F}=9950$ V/cm. The intermediate state is $5^2P_{3/2}$, $F=M_F=4$. A: $\sigma^+\sigma^-$ spectrum. B: $\sigma^+\pi$ spectrum. C: $\sigma^+\sigma^+$ spectrum. The resonances are labeled by the parabolic quantum numbers n, n_1, m_l.

TABLE I. The most excited states in the spectrum of hydrogen in the presence of the field $\mathcal{F}=9950$ V/cm. The states are labeled by the parabolic quantum numbers (n,n_1,m_l). E_R is the position of the state with respect to the zero-field-ionization limit. Γ is the width of the state and $C_{n_1}^{m_l}$ is the maximum value of the partial density of the state.[4] $[a(-N)\equiv a\times10^{-N}.]$

n,	n_1,	m_l	E_R (cm^{-1})	Γ (cm^{-1})	$(C_{n_1}^{m_l})^{1/2}$
21	20	0	−20.98	3.47	0.1678(−5)
20[a]	19	0	−64.66	0.568	0.382(−5)
20	18	0	−95.36	4.03	0.1753(−5)
19[a]	18	0	−110.77	8.62×10^{-3}	0.4009(−4)
19[a]	17	0	−139.20	0.270	0.6342(−5)
18[a]	17	0	−162.39	4.69×10^{-6}	0.2074(−2)
19	16	0	−167.86	1.58	0.2061(−5)
18[a]	16	0	−187.73	5.51×10^{-4}	0.1831(−3)
18[a]	15	0	−213.23	1.47×10^{-2}	0.3342(−4)
20	18	1	−80.04	1.63	0.344(−6)
19[a]	17	1	−124.73	0.056	0.257(−5)
20	17	2	−94.28	3.78	0.1480(−7)
19	16	2	−138.52	0.18	0.8157(−7)
19	15	2	−167.26	1.34	0.4976(−7)
18[a]	15	2	−187.36	3.12×10^{-4}	0.3108(−5)

[a]Identified structures in the Stark photoionization spectra from the state $5^5P_{3/2}$ $m_l=1$ of rubidium.

given spectrum in two different groups, the resonances of the same group having similar profiles. Furthermore, one can compare the present results to those obtained in a similar experiment and for the same electric field strength with the sodium atom.[8] It is then to be noticed that, in a given energy range, the structures are twice as numerous in the rubidium atom as in the sodium atom, provided that the Earth's magnetic field has been cancelled.

In the sodium atom we have identified all observed structures by using the parabolic quantum numbers n, n_1, m_l occurring in the hydrogenic model.[9] In this experiment the orbital magnetic quantum number m_l remains a good quantum number, and each structure in photoionization spectra corresponds to a well-defined m_l value: The $\sigma^+\sigma^-$, $\sigma^+\pi$, and $\sigma^+\sigma^+$ spectra correspond, respectively, to final states $m_l=0$, 1, and 2. In the analysis of rubidium spectra, if one supposes that m_l is an exact quantum number, only one resonance out of two can be identified in each spectrum; more precisely, only broader structures can be labeled.

However, keeping in mind that there exists an apparent degeneracy in the structures of the three rubidium spectra and that rubidium is a heavy atom, it is reasonable to assert that the symmetry breaking with respect to m_l arises from the spin-orbit interaction, which mixes excited states with the same m_j value but with two different m_l values ($m_l=m_j\mp\frac{1}{2}$). With this assumption, the structures of the $\sigma^+\sigma^-$ spectrum correspond to final states $m_j=\frac{1}{2}$ associated with the two series $m_s=\frac{1}{2}$, $m_l=0$ and $m_s=-\frac{1}{2}, m_l=1$. Similarly, in the $\sigma^+\pi$ spectrum, one observes $m_j=\frac{3}{2}$ states corresponding to the series $\frac{1}{2},1$ and $-\frac{1}{2},2$; lastly, $m_j=\frac{5}{2}$ states and $\frac{1}{2},2$ and $-\frac{1}{2},3$ series are to be considered in the analysis of the $\sigma^+\sigma^+$ spectrum. All structures observed in the three spectra can be labeled by using the hydrogenic model. In each spectrum the two series correspond to different m_s values: the broad resonances being associated with $m_s=\frac{1}{2}$ while the narrow ones correspond to $m_s=-\frac{1}{2}$. Identifications of the structures are written in Fig. 1.

Let us recall that in the photoionization spectra of the state $5^2P_{3/2}$, $m_s'=\frac{1}{2}$, $m_l'=1$, $m_j'=\frac{3}{2}$, one reaches final states with quantum number $m_j=\frac{1}{2}$, $\frac{3}{2}$, or $\frac{5}{2}$ accordingly as the polarization of the photoionizing light is of the type σ^-, π, or σ^+. In the final states only states with $m_s=\frac{1}{2}$ can be excited by direct absorption because the transition operator is spin independent.

The experimental study of the photoionization Stark spectra of the state $5^2P_{3/2}$, $F=4$, $M_F=4$ of the rubidium atom has made it obvious that the spin-orbit interaction strongly perturbs the spectra in the vicinity of the zero-field-ionization limit. Indeed, even if it is weak, this coupling is sufficient to lead to the appearance of additional structures in the photoionization spectra.

III. ANALYSIS OF THE DIFFERENT PROFILES OBSERVED IN THE RUBIDIUM STARK PHOTOIONIZATION SPECTRA

As said before, in the analysis of the photoionization spectra of the rubidium atom we have been led to assign the same set of parabolic quantum numbers (n,n_1,m_l) to two resonances in spite of their different profiles and widths; the first one belongs to the spectrum $m_j=m_l+\frac{1}{2}$, whereas the second one belongs to the spectrum $m_j=m_l-\frac{1}{2}$. For example, the $m_l=1$ resonances appear as narrow structures in the $\sigma^+\sigma^-$ spectrum, but they appear as broad structures in the $\sigma^+\pi$ spectrum. However, as has been shown previously[3,7] for interpreting the photoionization spectra, the most important quantity to be considered is the oscillator strength density rather than simply the density of excited states. Indeed, the oscillator strength density is a nondiagonal quantity involving the overlap of two different wave functions, so important interference effects may appear in its calculation. Consequently, the energy dependence of the density of oscillator strengths can strongly differ from that of the density of excited states.

A. Interpretation of the different profiles observed in the Stark photoionization spectra of rubidium

The main characteristics of the profiles observed in the rubidium Stark photoionization spectra can be interpreted qualitatively as discussed below. In the nonrelativistic hydrogenic approximation (Hamiltonian H_0), and in the vicinity of the zero-field-ionization limit, the Stark spectrum consists in discrete states labeled n,n_1,m_l,m_s and in continua labeled E,n_1,m_l,m_s. In the rubidium spectrum these different states are coupled either through the non-Coulombic part ΔV of the central potential or through the spin-orbit interaction Λ. The interaction ΔV couples only those states having the same m_l and m_s values; the matrix elements of this interaction are related to the quantum defects $\Delta_l\simeq -n^3\Delta V_{nl}$ of the unperturbed atom for states $l\geq|m_l|$. Indeed, if the exact electrostatic energy E_{nl} of a Rydberg state n,l,m_l,m_s can be obtained within the first-order perturbation theory, one can write

$$E_{nl}=\frac{-1}{2n^2}+\langle n,l,m_l,m_s\,|\,\Delta V\,|\,n,l,m_l,m_s\rangle$$
$$=\frac{-1}{2n^2}+\Delta V_{nl}\simeq\frac{-1}{2n^2}-\frac{\Delta_l}{n^3}\,. \tag{1}$$

From this equation it is obvious that ΔV_{nl} is negative. The spin-orbit interaction Λ couples the states having the same $m_j=m_l+m_s$ value. For a given m_j value, discrete and continuum states $m_{l+}=m_j-\frac{1}{2}, m_{s+}=\frac{1}{2}$ and $m_{l-}=m_j+\frac{1}{2}, m_{s-}=-\frac{1}{2}$ are mixed by the interaction Λ. The matrix elements of this interaction can be expressed in terms of the spin-orbit integrals $\xi_l=n^3\xi_{nl}$ which are positive. Indeed, one can write, if $|m_l|\leq l$,

$$\langle n,l,m_l,m_s\,|\,\Lambda\,|\,n,l,m_l,m_s\rangle=\frac{\xi_l}{n^3}m_lm_s$$

and (2)

$$\langle n,l,m_l,-\tfrac{1}{2}\,|\,\Lambda\,|\,n,l,m_l-1,\tfrac{1}{2}\rangle$$
$$=\frac{\xi_l}{n^3}[l(l+1)-m_l(m_l-1)]^{1/2}\,.$$

These relations obtained for the discrete states of the unperturbed atom can be generalized to the study of continuum states describing the atom in the presence of an external electric field by replacing $1/n^3$ by the density of continuum states with energy E.

The exact wave functions $\Phi(\alpha;m_j,E)$ of the total Hamiltonian corresponding to the energy E and to the quantum number m_j can be written as

$$\Phi(\alpha;m_j,E)=\sum_d a_d^+(\alpha;m_j,E)\varphi_d^+ + \sum_d a_d^-(\alpha;m_j,E)\varphi_d^- + \sum_{n_1}\int b_{n_1E'}^+(\alpha;m_j,E)\Psi_{n_1E'}^+ dE' + \sum_{n_1}\int b_{n_1E'}^-(\alpha;m_j,E)\Psi_{n_1,E'}^- dE' , \quad (3)$$

where φ_d^+ and φ_d^- are wave functions for discrete states m_{l+},m_{s+} and m_{l-},m_{s-}, respectively. The sums over d include the different discrete states characterized by the quantum numbers n and n_1. The wave functions $\Psi_{n_1E'}^+$ and $\Psi_{n_1E'}^-$ are associated with the continuum states of energy E', with parabolic quantum number n_1 and with quantum numbers m_{l+},m_{s+} and m_{l-},m_{s-}, respectively. The index α is used to characterize the different degenerate orthogonal and normalized eigenstates of the total Hamiltonian

$$\langle \Phi(\alpha;m_j,E) \mid \Phi(\alpha';m_j',E')\rangle = \delta_{\alpha\alpha'}\delta_{m_j,m_j'}\delta(E-E') . \quad (4)$$

For a discrete set of eigenstates of H_0 —N_+ and N_- discrete states φ_d^+ and φ_d^-, respectively, and M_+ and M_- continuum states $\Psi_{n_1E}^+$ and $\Psi_{n_1E}^-$, respectively—the exact wave functions $\Phi(\alpha;m_j,E)$ can be constructed using the diagonalization procedure introduced by Fano[12] and extended to include the interaction of the $N=N_++N_-$ discrete states with the $M=M_++M_-$ continua.[16]

It is possible to define $\mathscr{C}_{m_j}(E)$, the total density of states, with energy E and quantum number m_j in the continuous spectrum associated with the total Hamiltonian H. Indeed, for a continuous spectrum the amplitude in the asymptotic region of a normalized wave function is entirely determined and it varies regularly with the energy. On the contrary the probability of finding near the nucleus a state with quantum numbers m_j and E does not vary smoothly in the whole energy range; it represents the total density of states[4]

$$\mathscr{C}_{m_j}(E) \propto \sum_\alpha \mid \Phi(\alpha;m_j,E;\vec{r}) \mid^2, \quad \text{for } \mid \vec{r} \mid \text{ small} . \quad (5)$$

In the present problem, as the eigenvalues of the discrete states lie within the continua, the total density of perturbed states exhibits a resonance structure. If N discrete states are coupled to M continua, the number of resonances appearing in the density of states is at most equal to N, provided their widths are smaller than their spacings.

In the photoionization spectrum from a lower state g obtained with polarized light exciting only upper states with a given m_j value, the density of oscillator strengths is proportional to the squared matrix element of the transition operator T:

$$\frac{df(m_j,E)}{dE} \propto \sum_\alpha \mid \langle g \mid T \mid \Phi(\alpha;m_j,E)\rangle \mid^2 . \quad (6)$$

In the present study the lower state is $5^2P_{3/2}m_l'=1$, $m_s'=\frac{1}{2}$. As the operator T is not depending on the spin of the electron, only the states φ_d^+ and $\Psi_{n_1E'}^+$ can be excited directly from the ground state. Furthermore, the state g is localized in the vicinity of the nucleus; so $df(m_j,E)/dE$ is proportional to the total density of states $\mathscr{C}_{m_j}(E)$:

$$\frac{df(m_j,E)}{dE} = \mathscr{C}_{m_j}(E) I(g,\epsilon;E) . \quad (7)$$

The factor I which depends on the lower state g and on the polarization ϵ of the photoionizing light, modulates the density of states; it takes into account interference effects between the different photoexcitation channels introduced in the matrix element of the transition operator. Consequently, in order to interpret the number of resonances which appear in the photoionization spectrum of a given energy range it is necessary to explicitly take into account all of the discrete states present in this range, these states being excited either directly or indirectly from the lower state.

If one supposes that the different resonances are well resolved, the resonances can then be analyzed independently. The width $\Gamma_d^\pm$ of a resonance associated with a discrete state $\varphi_d^\pm$ of energy $E_d^\pm$ can be evaluated from the golden rule; it is given by the following relation which is valid for uncoupled continua:

$$\Gamma_d^\pm = 2\pi \sum_j \mid \langle \varphi_d^\pm \mid H \mid \varphi_{j,E'=E^\pm}\rangle \mid^2 . \quad (8)$$

The sum includes all the continua which are coupled to $\varphi_d^\pm$. The width Γ_d^+ (Γ_d^-) is given by the sum $\Delta V+\Lambda$, ΔV couples the discrete state φ_d^+ to the continua $\Psi_{n_1,E}^+$ (φ_d^- to $\Psi_{n_1,E}^-$), and the interaction Λ couples φ_d^+ (φ_d^-) to the continua $\Psi_{n_1,E}^+$ and $\Psi_{n_1,E}^-$. Consequently, in order to interpret the widths of the resonances it is necessary to introduce all the continua which are coupled to the discrete states, these continua being directly or indirectly excited from the lower state.

A given discrete state d_1 described by the set (n,n_1,m_l) can be observed in both spectra $m_j=m_l+\frac{1}{2}$ and $m_j=m_l-\frac{1}{2}$; the profiles associated with these two resonances $\varphi_{d_1}^+$ and $\varphi_{d_1}^-$ can be different inasmuch as their widths $\Gamma_{d_1}^\pm$ or their Fano parameters $q_{d_1}^\pm$ are not identical. If the spin-orbit interaction is smaller than the electrostatic interaction, the widths $\Gamma_{d_1}^+$ and $\Gamma_{d_1}^-$ are nearly equal. But if these two interactions are of the same order of magnitude, their contributions interfere constructively in the calculation of $\Gamma_{d_1}^-$ but destructively for $\Gamma_{d_1}^+$ if m_l is positive [see Eqs. (1) and (2)]: In this case $\Gamma_{d_1}^+$ and $\Gamma_{d_1}^-$ are very different. The parameter $q_{d_1}^+$ depends simultaneously on the width of the state $\Gamma_{d_1}^+$ and on the matrix elements D and d of the operator T connecting the lower state g to

$\varphi_{d_1}^+$ and $\Psi_{n_1,E}^+$, respectively; the parameter $q_{d_1}^+$ being nonvanishing, the resonance $\varphi_{d_1}^+$ exhibits a typical Fano profile. For the resonance $\varphi_{d_1}^-$, the Fano parameter $q_{d_1}^-$ vanishes, this state not being directly excited from the lower state; then $\varphi_{d_1}^-$ appears as an "absorption hole" in the photoionization spectrum.

It is also possible to compare the widths of the two series of resonances $\varphi_{d_+}^+$ and $\varphi_{d_-}^-$ observed in a given spectrum m_j. If the electrostatic interaction ΔV is larger than the spin-orbit interaction Λ, then the resonance $\varphi_{d_+}^+$ is larger than the resonance $\varphi_{d_-}^-$. Indeed, the widths are directly related, respectively, to the quantum defects $\Delta_{m_j-1/2}$ and $\Delta_{m_j+1/2}$ which verify $\Delta_{m_j-1/2}>\Delta_{m_j+1/2}$, Δ_l decreasing with increasing l value. This feature has been observed in the analysis of the $\sigma^+\sigma^-$ and $\sigma^+\pi$ spectra of rubidium.

B. Model calculation

In the energy range $E\sim -200\ \mathrm{cm}^{-1}$ the resonances of the type φ^+ are located between two structures associated with discrete states of the type φ^-. In order to interpret quantitatively the recorded profiles, we introduce a simple model involving two series of $N_+=N_-=3$ discrete states of the type φ^+ and φ^-, respectively. These states are coupled to the two continua Ψ_E^+ and Ψ_E^-. Indeed, the interactions ΔV or Λ which couple discrete $\varphi_d^\pm$ states and continuum $\Psi_{n_1,E}^\pm$ states are short-range interactions and it is possible to factorize the matrix elements as follows:

$$\langle \varphi_d^+ \mid \Delta V \mid \Psi_{n_1,E}^+ \rangle = v_d^+ \omega_{n_1,E}^+ ,$$

$$\langle \varphi_d^+ \mid \Lambda \mid \Psi_{n_1,E}^+ \rangle = \lambda_d^{+\,+} \omega_{n_1,E}^+ ,$$

and

$$\langle \varphi_d^+ \mid \Lambda \mid \Psi_{n_1,E}^- \rangle = \lambda_d^{+\,-} \omega_{n_1,E}^- \tag{9}$$

with

$$\sum_{n_1} (\omega_{n_1,E}^+)^2 = \sum_{n_1} (\omega_{n_1,E}^-)^2 = 1 .$$

Similar equations can be written for the states φ_d^-. Then it is equivalent to state that all resonances interact with just two continua[16]:

$$\Psi_E^+ = \sum_{n_1} \omega_{n_1,E}^+ \Psi_{n_1,E}^+$$

and (10)

$$\Psi_E^- = \sum_{n_1} \omega_{n_1,E}^- \Psi_{n_1,E}^- .$$

The matrix elements of the interaction which couple the discrete states $\varphi_d^\pm$ to the continua Ψ_E^+ and Ψ_E^- can be written as follows:

$$\langle \varphi_d^+ \mid \Delta V + \Lambda \mid \Psi_E^+ \rangle = v_d^+ + \lambda_d^{+\,+} = V_1 ,$$

$$\langle \varphi_d^+ \mid \Lambda \mid \Psi_E^- \rangle = \lambda_d^{+\,-} = V_2 ,$$

$$\langle \varphi_d^- \mid \Lambda \mid \Psi_E^+ \rangle = \lambda_d^{-\,+} = W_1 ,$$

$$\langle \varphi_d^- \mid \Delta V + \Lambda \mid \Psi_E^- \rangle = v_d^- + \lambda_d^{-\,-} = W_2 .$$

The states Ψ_E^+ and φ^+ can be excited directly from the ground state g, and the matrix elements are written as

$$\langle g \mid T \mid \varphi_d^+ \rangle = D, \quad \langle g \mid T \mid \Psi_E^+ \rangle = d .$$

For all states belonging to the same series we suppose that the strengths of the coupling with a given continuum are equal and that their probability of excitation from the lower state is the same. No coupling between the discrete states has been introduced because these interactions can be neglected if their strengths are much smaller than the energy difference between the two discrete states. We also neglect the coupling of the two continua due to the spin-orbit interaction. Indeed, far from the nucleus the amplitudes of the continuum wave functions are large, but in this region the strength of the spin-orbit interaction decreases rapidly (as $1/r^3$); consequently, $\langle \Psi_E^+ \mid \Lambda \mid \Psi_E^- \rangle \ll 1$. Furthermore, the strengths of this coupling can be related to the coefficients δ, $\lambda_d^{+\,-}$, and $\lambda_d^{-\,+}$ inasmuch as continua correspond to quasidiscrete states for which the field-ionization process cannot be neglected; then the broadening of these states is at least equal to their spacing δ. In this approximation we have verified that the introduction of the coupling between the two continua does not modify the calculated profiles.[17]

The studied model is presented in Fig. 2. For a given set of parameters (E_i, V_i, W_i, d, and D) the total density of oscillator strengths df/dE is calculated according to the method described by Fano.[12] The total density of states $\mathscr{C}(E)$ is related to the quantity

$$D(E) = \sum_{d,\alpha} [\, |\, a_d^+(\alpha,E)\,|^2 + |\, a_d^-(\alpha,E)\,|^2] .$$

For a given energy E, $D(E)$ is equal to the total weight

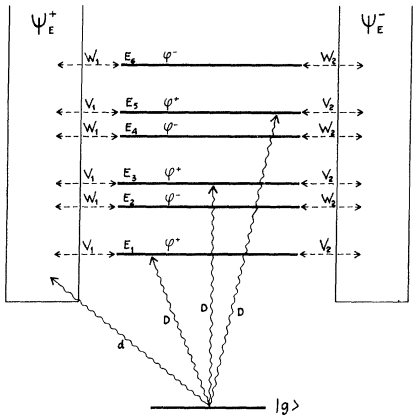

FIG. 2. Schematic representation of the different discrete and continuous excited Stark states with a given m_j value ($m_j=\frac{1}{2}$, $\frac{3}{2}$, or $\frac{5}{2}$). The mutual couplings are due to the following: ΔV, the non-Coulombic part of the central potential; Λ, the spin-orbit interaction. These states are excited from the intermediate state $5^2P_{3/2}$, $m_l'=1$, $m_s'=\frac{1}{2}\equiv g$ of the ^{85}Rb atom through electric dipole transitions (d and D).

of the discrete states of energy E in the exact wave functions $\Phi(\alpha;E)$ of total energy E [Eq. (3)]; $D(E)$ shows how the discrete states are "diluted" in the actual stationary states of the continuum spectrum because of their coupling with the unperturbed continuum states. The energy dependence of $D(E)$ and df/dE can be very different; indeed, $D(E)$ characterizes the autoionization phenomenon while df/dE introduces supplementary interference effects associated with the photoionization process and depending on the matrix elements d and D of the transition operator. In the studied examples the resonances observed in the density of states are rather well resolved; their individual width are nearly equal to the value obtained from the golden rule. However, important interference effects occur in the calculation of the density of oscillator strengths, which proves that the different resonances cannot be studied independently. Some results are presented in Fig. 3.

In the $\sigma_+\sigma_-$ spectrum, upper states $m_j=\frac{1}{2}$ are excited. The discrete states φ^+ ($m_l=0$, $m_s=\frac{1}{2}$) are coupled to the continuum Ψ_E^+ through the non-Coulombic part of the central potential ΔV, and V_1 is mainly related to the quantum defect Δ_s which is large.[17] The discrete states φ^- ($m_l=1$, $m_s=-\frac{1}{2}$) are coupled to the continuum Ψ_E^- through interactions ΔV and Λ; consequently, W_2 can be expressed in terms of Δ_p and ξ_p. As the quantum defects Δ_l are decreasing with increasing l, one can suppose that $|V_1|>|W_2|$. States associated with different m_s values, φ^+ and Ψ_E^- or φ^- and Ψ_E^+, are coupled through the spin-orbit interaction and the couplings $V_2=W_1$ can be expressed in terms of ξ_p. Furthermore, taking into account Eqs. (1) and (2), one can suppose that V_1 and W_2 are negative and V_2 and W_1 are positive. Both states and oscillator strength densities have been calculated for the following set of parameters:

$$E_3-E_1=E_4-E_2=3.0\ ,\quad E_2-E_1=2.0\ ,$$

$$V_1=-0.2828\ ,\quad W_2=-0.1728\ \text{(arbitrary units)}\ ,$$

$$V_2=W_1=0.1414\ ,$$

$$d=1.0,\quad D=0.3\ .$$

In this approximation, for isolated resonances, the Fano parameters are equal to $q_+=0.3377$, $q_-=0.0$. The oscillator strength density consists of broad slightly dissymmetric structures separated by a symmetric three times narrower resonance. The intensities of the different resonances do not differ strongly. The calculated photoionization spectrum reproduces rather well the experimental structure observed in the $\sigma^+\sigma^-$ spectrum in the vicinity of the resonance $n=17$, $n_1=15$, $m_l=1$, $m_s=-\frac{1}{2}$ (see Fig. 1).

The structures observed in the $\sigma^+\sigma^+$ spectrum correspond to states $m_j=\frac{5}{2}$ classified according to the two series $m_l=2, m_s=\frac{1}{2}$ and $m_l=3, m_s=-\frac{1}{2}$. The quantum defect Δ_l and the spin-orbit interaction decrease with increasing l. In order to interpret the structures observed in the $\sigma^+\sigma^+$ spectrum, we suppose that ΔV and Γ are of the same order of magnitude and we choose the following parameters:

$$E_3-E_1=E_4-E_2=3.0\ ,\quad E_2-E_1=2.4\ ,$$

$$V_1=-0.1414,\quad W_2=-0.1\ ,$$

$$V_2=W_1=0.1,\quad \text{(arbitrary units)}$$

$$d=1.0,\quad D=0.37\ .$$

With this set of parameters $q_+=0.83$, $q_-=0$.

The calculated spectrum consists of very asymmetric structures separated by a less intense symmetric, and narrow resonance. It reproduces rather well the experimental profile in the vicinity of the resonance $n=16$, $n_1=12$, $m_l=3$, $m_s=-\frac{1}{2}$.

In the analysis of these spectra it has been necessary to take into account both the non-Coulombic character of the central potential and the spin-orbit interaction. However, the relative importance of these two interactions is not the same according to each studied spectrum. Furthermore, this analysis clearly demonstrates that in a photoionization spectrum the density of oscillator strengths depends strongly on the excitation process (i.e., on d and D) and differs greatly from the density of upper states.

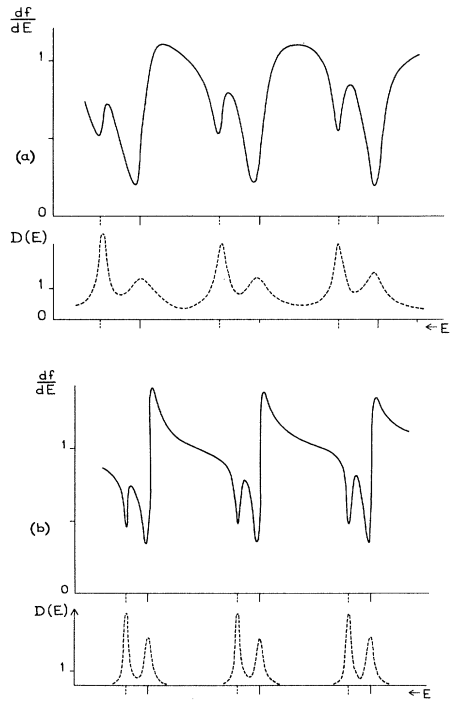

FIG. 3. Calculated density of discrete states $D(E)$ and density of oscillator strengths df/dE obtained in a simple model consisting of two series φ^+ and φ^- involving three excited discrete states coupled to two continua Ψ_E^+ and Ψ_E^-. The individual resonances are characterized by their energies E_i indicated by the solid curve for φ^+ states and the dashed curve for the φ^- states. The states φ^- and Ψ_E^- cannot be excited directly from the ground state. (a) $\sigma_+\sigma_-$ spectrum; (b) $\sigma_+\sigma_+$ spectrum.

IV. DISCUSSION: OBSERVATION OF FANO PROFILES IN THE STARK PHOTOIONIZATION SPECTRA OF ALKALI ATOMS

In this simple model discussed above, it has been shown that the states $m_s=-\frac{1}{2}$, which cannot be populated

directly by absorption from the lower state $5^2P_{3/2}$ $m_l'=1$, $m_s'=\frac{1}{2}$, are associated to additional structures in the photoionization spectra. These resonances look like symmetric peaks but they are not located at the energy E^- of the discrete state (see Fig. 3). These structures correspond actually to holes in the absorption curve ($q^-=0$), and these minima are cut out in the large profiles corresponding to the resonances φ^+. The width Γ^- does not correspond to the width of the symmetric peak, but it is directly related to the width of the hole centered at E^-. This discussion demonstrates how difficult it is to analyze an absorption spectrum in which numerous resonances appear. If the widths of the resonances are of the same order of magnitude as the energy difference between two consecutive discrete states, there are interference effects between the different profiles in the calculation of the transition matrix elements and the structures cannot be studied independently.

In the energy range located between the classical field-ionization limit E_c and the zero-field-ionization limit E_0, the Stark spectrum of hydrogen consists of quasidiscrete states superimposed to ionization continua. In alkali-metal atoms, asymmetric peaks, characteristic of the interaction between a discrete state and a continuum, are thus expected to appear. However, typical Fano profiles are not so numerous in the experimental spectra; indeed, such profiles, described by the well-known analytical formula [Eq. (21) of Ref. 12], are observed if only single states interact with continua and if these interactions can be regarded as independent of the energy over a sufficiently large range.

Near E_c, in the hydrogen model, there are few continua associated with small n_1 values. Between the $n_1=0$ and $n_1=1$ parabolic ionization thresholds[4] associated with a chosen m_l value, only one continuum is to be considered, and the theoretical analysis is much more simple. However, in this energy range quasidiscrete states are very numerous; for example, for $\mathcal{F}=2189$ V/cm, the first two parabolic ionization thresholds $m_l=0$ are separated by 5.4 cm^{-1} and in this energy range there are six quasidiscrete states $m_l=0$. Consequently, in a nonhydrogenic system these discrete states are associated with typical Fano profiles as long as the coupling between discrete and continuum states is sufficiently weak. Fano profiles could probably be observed in similar conditions in the lithium spectrum. Indeed, the theoretical width, calculated by taking into account the non-Coulombic part of the electrostatic potential, is approximately equal to 0.07 cm^{-1}. Let us remark that the asymmetry of these narrow profiles should be observed experimentally provided that high-resolution techniques be used. The corresponding widths in the sodium atom are of the order of 1 cm^{-1}; therefore, it is not possible in this atom to analyze the structures independently because interference effects exist between the different resonances. In the rubidium atom[13] Fano profiles due to the spin-orbit interaction could probably be observed in this energy range $E\sim E_c$.

Near the zero-field-ionization limit, quasidiscrete states are not numerous and typical Fano profiles are frequently observed, especially in light alkali-metal atoms such as sodium,[7,8] for which the non-Coulombic character of the central potential ΔV is not too large. However, let us remark that a quasi-discrete state which possesses in the hydrogenic approximation a non negligible ionization width, cannot correspond in a non-hydrogenic spectrum to a structure having a typical Fano profile [Eq. (21) of Ref. 12] because it is not possible to neglect the energy dependence of the coupling between the quasidiscrete state and the continua. The theoretical calculation of the resulting profiles in this energy range is relatively difficult because numerous continua must be taken into account. Furthermore, it is necessary to express the coupling between different continua and between different energy eigenfunctions within each continuum.[18] This procedure has been successfully applied to the analysis of the Stark two-step photoionization spectrum through the 3^2P term of sodium.[18] For this atom it is possible to study only one single discrete state. An alternative different approach does not consider the different resonances independently, but it directly calculates the photoionization probability versus the wavelength of the photoionizing light.[5] This method, developed within the framework of the multichannel quantum-defect theory, separately considers the short-range interaction ΔV and the long-range interaction associated with the Coulomb-Stark potential, and introduces the contributions due to the spherically symmetric ionic core in terms of quantum defects. These two methods do not take into account the spin-orbit interaction. It will be very interesting to extend both methods to obtain quantitative results concerning the Stark photoionization spectra of heavy alkali-metal atoms.

[1]R. R. Freeman, N. P. Economou, G. C. Bjorklund, and K. T. Lu, Phys. Rev. Lett. 41, 1463 (1978).
[2]R. R. Freeman and N. P. Economou, Phys. Rev. A 20, 2356 (1979).
[3]E. Luc-Koenig and A. Bachelier, Phys. Rev. Lett. 43, 921 (1979).
[4]E. Luc-Koenig and A. Bachelier, J. Phys. B 13, 1743; 13, 1769 (1980).
[5]D. A. Harmin, Phys. Rev. Lett. 49, 128 (1982); Phys. Rev. A 26, 2656 (1982).
[6]W. Sander, K. A. Safinya, and T. F. Gallagher, Phys. Rev. A 23, 2448 (1981).
[7]Ting Shan Luk, L. Di Mauro, T. Bergeman, and H. Metcalf, Phys. Rev. Lett. 47, 83 (1981).
[8]S. Feneuille, S. Liberman, E. Luc-Koenig, J. Pinard, and A. Taleb, Phys. Rev. A 25, 2853 (1982).
[9]H. A. Bethe and E. E. Salpeter, *Quantum Mechanics of One- and Two-Electron Atoms* (Academic, New York, 1957).
[10]G. J. Hatton, Phys. Rev. A 16, 1347 (1977).
[11]M. G. Littman, M. M. Kash, and D. Kleppner, Phys. Rev.

Lett. 41, 103 (1978).
[12]U. Fano, Phys. Rev. 124, 1866 (1961).
[13]S. Feneuille, S. Liberman, J. Pinard, and A. Taleb, Phys. Rev. Lett. 42, 1404 (1979).
[14]S. Feneuille, S. Liberman, E. Luc-Koenig, J. Pinard, and A. Taleb, J. Phys. B 15, 1205 (1982).
[15]T. F. Gallagher, B. E. Perry, K. A. Safinya, and W. Sandner, Phys. Rev. A 24, 3249 (1981).
[16]F. H. Mies, Phys. Rev. 175, 164 (1968).
[17]J. M. Lecomte, Thèse de Troisième Cycle, Université de Paris—Sud, Orsay 1983 (unpublished).
[18]L. Di Mauro, T. Bergeman, P. McNicholl, and H. Metcalf, J. Phys. (Paris) Colloq. 43, C2-167 (1982).